Advances in Science and Technology Research Journal

Advances in Science and Technology Research Journal 2023, 17(6), 49–62
https://doi.org/10.12913/22998624/173562
ISSN 2299-8624, License CC-BY 4.0

Received: 2023.08.08
Accepted: 2023.10.09
Published: 2023.11.21

Analysis and Investigation the Effect of the Printing Parameters on the Mechanical and Physical Properties of PLA Parts Fabricated via FDM Printing

Hind H. Abdulridha[1*], Tahseen F. Abbas[1]

[1] Production Engineering and Metallurgy Department, University of Technology-Iraq, Baghdad, Iraq

* Corresponding author's email: Hind.H.Abdulridha@uotechnology.edu.iq

ABSTRACT

Fused deposition modeling (FDM) is a commonly used additive manufacturing (AM) technique that creates prototypes and parts with intricate geometrical designs. It is gaining popularity since it enhances products by removing the need for expensive equipment. The printed item's mechanical properties are affected by the type of materials used, the printing process, and the printing parameters. The 3-D model of the polylactic acid (PLA) filament generated specimens was created using the Fused Deposition Modeling procedure and developed using Solid Works. This study investigates the effect of printing parameters on the mechanical and physical properties of samples printed using a Fused Deposition Modeling machine (Creality Ender-5 Pro). Six parameters are used: infill pattern, density, overlap percentage, layer thickness, shell thickness, and top/bottom layer number. Five levels were chosen for each FDM parameter. The results illustrated how printing parameters affected the mechanical and physical properties of samples, which were proven by ultimate tensile stress, surface roughness, and percentage of tensile average deviation. A comparison between the predicted results and the measured results was presented, and the maximum percentage error of the model, which fit the data well, was 0.54%, 0.3%, and 1.36% for ultimate tensile strength (UTS), surface roughness (Ra), and Tensile average deviation percentage respectively.

Keywords: fused deposition modeling, PLA, process parameters, tensile strength.

INTRODUCTION

Metals and polymers have been processed using a novel manufacturing technique known as additive manufacturing (AM), also referred to as 3D printing. AM is the technique of combining materials (usually layer by layer) with the assistance of 3D data. The advantages of the AM method include lower prototyping costs, quicker, less expensive production runs, and fewer inventories on hand, while the drawbacks include high production expenses, a slow build rate, and a limited range of component sizes. The use of additive manufacturing in current industries such as automotive sector development, arts and design development, aerospace and biomedical applications, and architecture has expanded because of its versatility and low cost in creating complicated designs. Currently, the electronics, aerospace, and biomedical industries all heavily rely on AM techniques. Plastic sheet lamination (PSL), selective laser sintering (SLS), fused deposition modeling (FDM), selective laser melting (SLM), and laminated object manufacturing (LOM) are the different AM techniques [1]. Due to their simplicity of production, low cost, and great performance, polymers are the most widely used materials in many applications [1–3]. The two alternative classifications for fused filament fabrication (FFF) that are most frequently used are fused deposition modeling (FDM) and three-dimensional printing (3DP). Due to the ease of the deposition process, the variety of materials on the market, the low cost of printer equipment, and the wide selection of inexpensive filaments, this approach is the most widely utilized of all

AM methods. In environmentally friendly applications, a variety of cutting-edge materials and colors are regularly used, including wood for clothes, design, and furniture [4].

Numerous studies that were published made an effort to raise the production parameters for fused deposition modeling in order to produce parts of high quality. For instance, Mohd et al. (2022) [5] examined the optimum FDM printing parameters (printing speed, orientation, infill density, and layer thickness) utilizing thermoplastic composites supplemented with oil palm fiber that affect flexural strength, Young's modulus, and tensile strength. The findings demonstrate that the optimum printing conditions were flat orientation, 0.4 mm layer thickness, 10 mm/s printing speed, and 50% density. Menderes et al. (2022) [6] determined the impacts of FDM process parameters (filling structures, occupancy rates, and table orientation) on the PLA mechanical characteristics. According to the findings, tensile strength and izod impact values have a direct relationship with occupancy rate. The estimating model's discrepancy with the experimental findings did not exceed the maximum value of 1.8%. Maria et al. (2022) [7] investigated the impact of different infill patterns (Lines, Grid, Tri-Hexagon, Triangles, Zigzag, Gyroid, Cubic, Octet, and Concentric) on the PLA parts tensile strength. According to the findings, the triangle infill pattern has a lower tensile strength of 21 MPa than the concentric infill pattern, which has a greater tensile strength of 32.174 MPa. Tahseen et al. (2022) [8] investigated the impacts of FDM parameters (outer shell width, layer thickness, infill density, and pattern) on the PLA compressive property. The results confirmed that infill density has a higher impact on compressive resistance, while layer thickness has no impact on compressive resistance. R.A. et al. (2021) [9] analyzed the tensile strength of PLA-printed items made from red, blue, and yellow primer filaments to determine the most significant parameters (layer thickness, printing temperature, and printing speed) and their interactions with the tensile strength. From these findings, it has been illustrated that process parameters have a greater impact than filament colors do, with layer thickness having the greatest impact on tensile strength. In 2021, Selim et al. [10] examined how process parameters affected the PLA specimen's tensile strength when fabricated using FDM. In the investigation, a 100% density rate produced a larger tensile stress than a density rate of 20%. By comparing the specimens with a 20% density rate to one another, the Grid-patterned specimen had the highest recorded tensile stress value. The cross-3D-patterned sample was found to have the closest specific strength to the full-filled sample. Mohd et al. (2021) [11] studied the impact of three pressing mechanisms (roller, ball, and press) on 3D printing components. They found that roller pressing has a better effect on FDM components and can improve tensile strength and surface roughness when integrated with a 3D printer. This suggests that roller mechanisms could be used as integrated pressing tools to enhance 3D printer properties. The combined infill patterns (honeycomb, solid, grid, wiggle, and rectilinear) that affect tensile characteristics in 3D printed objects were examined by Mohammadreza et al. (2020) [12]. The results showed that grid and honeycomb have greater strength while having lighter weights than solids. In this investigation, strength declines as build orientation increases. Digital image correlation (DIC) was used by Can et al. (2020) [13] to investigate the impact of process parameters on the yield strength, elastic modulus, densification strain, plastic platform stress, and tensile strength of printed PLA lattice structures. According to the experimental findings, the elastic modulus and tensile strength increase as the temperature of printing increases, while plastic platform stress, yield strength, and densification strain decrease as the speed of printing increases. The impact of the initial FDM parameters, such as layer height, infill percentage, and raster orientation, on the mechanical properties of thermoplastic polyurethane at a high strain rate (2500 s1) was described by Muhammad et al. (2020) [14]. Layer height was discovered to be the most important component at a quasi-static rate of loading (improvement in tensile strength). The resulting tensile strength of the sample decreased when the layer height of the sample increased. According to Teng et al. (2020) [15], a filament made of a wood fiber-polylactic acid composite (WPC) feedstock was utilized to print the specimen using FDM. The findings demonstrate that the printed WPC part's density grew as printing speed decreased, but its surface color darkened in comparison to parts fabricated at a high speed. These findings demonstrate that the surface roughness, density, surface color, and compressive characteristics of

the fabricated part are significantly affected by the printing speed. In 2020, Cristina et al. [16] examined the impacts of size effect (various thicknesses) and spatial printing direction on the tensile characteristics of FDM parts. Spatial orientation was found to have a higher impact on tensile strength and a smaller impact on young modulus. Additionally, the tensile strength and Young modulus both decrease as the number of layers increases.

The physical and mechanical properties of the parts produced with the FDM system vary depending on the specified parameters of the printing process. Due to the values of the selected printing parameters, which have significant effects on the mechanical and physical properties of the produced samples, some printed samples have poor mechanical and physical properties. Therefore, the aim of the work is to determine how the infill density, pattern, overlap percentage, layer thickness, shell thickness, and top/bottom layer number affect the physical and mechanical properties of printed samples fabricated using the FDM method. Based on test results, the ultimate tensile strength (UTS), surface roughness (Ra), and average tensile deviation percentage of the specimens are evaluated and analyzed in order to recognize the variable values that influence the properties of printed specimens.

EXPERIMENTATION

Material and method

The effect of the FDM process parameters on mechanical and physical properties has been investigated in previous works [17–19]. The major objectives of this work were to demonstrate how infill pattern, density, overlap, layer thickness, shell thickness, and top/bottom layer number affect tensile strength, surface roughness, and dimensional accuracy. In order to examine the impact of these parameters on dog-bone specimens, physical and mechanical properties analysis were done in this work. This sample was created using FDM printers and constructed in accordance with ASTM D638 Type 4 standards.

The 3D model's geometry was created using a set of linked triangles in a standard triangle language (STL) file. This 3D design was transformed into the language of machines (G-Code) through the slicing process, making it ready for printing. The STL file was prepared using Ultimaker Cura 4.13.1 software to generate appropriate G-codes. Figure 1 (a, b) illustrates the part's solid work model (ASTM D638 Type 4) and its STL file, respectively. Table 1 lists the six input parameters and the various levels that were used to produce the PLA type TORWELL filaments.

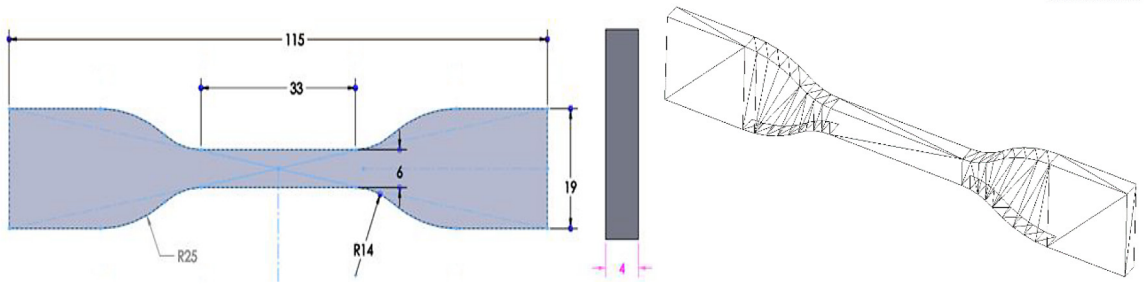

(a) (b)

Fig. 1. (a) Part SolidWorks Model (all dimensions in mm), (b) SolidWorks Model STL File

Table 1. FDM process parameters and their levels

FDM parameters	*Levels*				
	1	2	3	4	5
Infill density %	20	40	60	80	100
Infill pattern	Grid	Triangles	Cubic	Lines	Tri-Hexagon
Layer thickness	0.10	0.15	0.20	0.25	0.30
Shell thickness	0.4	0.8	1.2	1.6	2.0
Top/bottom layer no.	2	3	4	5	6
Infill overlap %	0	5	10	15	20

Fig. 2. Creality Ender-5 pro 3D printer

Table 2. FDM setup's specifications

No.	*Parameters*	*Values*
1	Layer thickness	100 – 400 Microns
2	Precision of print	+/- 100 microns
3	Max extruder temperature	260 °C
4	Nozzle size	0.4 mm (0.2 and 0.3 mm supported)
5	Filament type	ABS, TPU, PETG, PLA, Wood
6	Print bed	Heated bed with soft magnetic stickers
7	Max hotbed temperature	135 °C
8	Printing area	(220 * 220 * 300 mm)
9	Bed leveling	Manual
10	Display	LCD screen

Table 3. PLA filament specifications and properties

No.	*Parameters*	*Values*
1	Material	PLA with diameter of 1.75×10^3 µm
2	Length	330 $\times10^6$ µm
3	Weight	1 kg for each spool
4	Density	1.24 g/cm^3
5	Melt Flow Index	6 g/10 min, 190°C/2.16 kg
6	Heat Distortion Temp	50 °C
7	Tensile Strength	62 Kg/cm^2
8	Tensile Elongation	4.4%
9	Flexural Strength	66 Kg/cm^2
10	Flexural Modulus	28000 Kg/cm^2
11	Impact strength	4.2 KJ/m^2
12	Diameter Accuracy	1.75 mm: 1.70 ~ 1.78 mm

A Creality Ender-5 Pro 3D printer, as shown in Figure 2, was used to print all specimens. Table 2 contains a list of the FDM setup's specifications. A red polylactic acid (TORWELL PLA) filament with a 1.75 mm diameter was used as the work material due to its reliable properties. Table 3, contain the PLA material's specification and properties.

An influential, straightforward, and systematic technique is produced through the design of experiments utilizing the Taguchi method for identifying the ideal machining conditions in the production process. The Taguchi approach was utilized to construct the experiment. Six process parameters were used to examine how FDM parameters affected tensile strength: the percentage of density, infill pattern, layer thickness, shell thickness, number of top/bottom layers, and percentage of infill overlap. There are five levels of variation for each of these parameters. The Taguchi method was used to measure the performance characteristic that deviates from the required values by using the signal-to-noise S/N ratio.

In order to maximize (tensile strength) and minimize (Surface Roughness, tensile average deviation%), the higher-the-better tensile strength and the lower-the-better Surface roughness and dimensional accuracy should be selected. Equations 1 and 2 can be used to represent the S/N ratio for the higher-the-better, smaller-the-better performance characteristic:

- Larger is better:

$$\frac{S}{N} = -10\log\left(\frac{1}{n}\sum_{i=1}^{n}\frac{1}{y_i^2}\right) \tag{1}$$

- Smaller is better:

$$\frac{S}{N} = -10\log\left(\frac{1}{n}\sum_{i=1}^{n} y_i^2\right) \tag{2}$$

where: n – measurements total number;

y_i – the value of the characteristics that were measured.

The specimens were tested in accordance with ASTM D638 Type 4 standards on a WDW-200E computer-controlled electronic universal testing machine, as shown in Figure 3, to evaluate the mechanical properties of the fabricated specimens.

At room temperature, the testing was conducted at a controlled speed of 1.5 mm/min [16, 20]. Load, deformation, stroke, and time data were

Fig. 3. WDW-200E computer-controlled electronic universal testing machine

recorded during the experiments. The ultimate tensile strength was determined using the data that has been recorded. Based on the actual, not the CAD model, dimensions of each specimen, the stresses, and the mechanical properties can be determined. The tensile strength of each PLA test sample was estimated using equation 3. The various PLA filament test specimens are shown in Figure 4.

$$\sigma = \frac{F}{A} \tag{3}$$

where: σ – Tensile stress (N/mm^2);
F – Applied force (N);
A – cross-section area of fabricated part (mm^2).

Using a profile measurement device (Pocket Surf), the surface roughness of each tensile test sample was determined with 0.25 mm measurement distance as indicated in Figure 5. The surface roughness of the printed parts is represented by the average value that was calculated by performing the Ra calculation three times perpendicular to layers direction in different places on the same specimen.

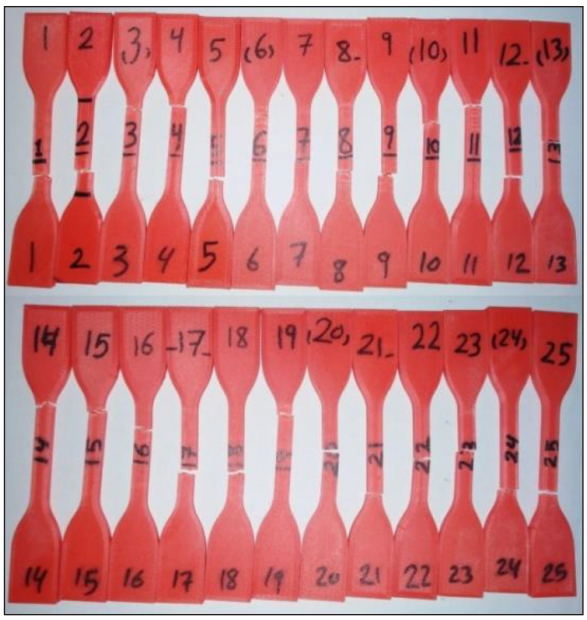

Fig. 4. PLA filament testing specimens

All of the molded specimens were measured and compared to the CAD model in order to evaluate the impact of the processing parameters on the tensile average deviation percentage (dimensional accuracy). Each specimen's measurements were taken using a digital vernier caliper. Every

Fig. 5. The surface roughness tester (Pocket Surf)

geometry was measured three times throughout each run, and using Equations (4-6), the average percentage deviation for the geometry was determined [21].

$$\text{Deviation } (D_i) = \left|\begin{matrix}\text{Specified Dimension} - \\ - \text{ Observed Value}\end{matrix}\right| \quad (4)$$

$$\text{Percentage Deviation } (D_{pi}) = \\ = \left(\frac{\text{Deviation (Di)}}{\text{Specified Dimension}}\right) * 100 \quad (5)$$

$$\text{Average Percentage Deviation} = \\ = \frac{D_{p1} + D_{p2} + D_{p3}}{3} \quad (6)$$

RESULTS AND DISCUSSION

The effects of six printing parameters on the ultimate tensile strength, surface roughness, and tensile average deviation percentage (dimensional accuracy) are shown in the results presented below. The experimental tensile strength, surface roughness, and dimensional accuracy data for 25 specimens are presented in Table 4.

Figure 6 show stress-strain diagram for 25 dog-bon specimen. In order to crack grid, triangle, Lines, cubic, and tri-hexagon patterns in dog-bone samples, a wide range of loads was applied. It has been shown that FDM specimens with the number 16 are strongest, among other parts, grid pattern with 80% density, 0.25 mm layer

Table 4. Ultimate tensile strength, surface roughness, and tensile average deviation % of printed parts

NO.	Infill density %	Infill pattern	Layer thickness (mm)	Shell thickness (mm)	Top/bottom layer no.	Infill overlap %	Ultimate tensile stress UTS (MPa)	Surface roughness Ra (μm)	Tensile average deviation %
1	20	Grid	0.10	0.4	2	0	10.8374	7.0608	0.556
2	20	Triangles	0.15	0.8	3	5	29.2921	9.2713	0.806
3	20	Cubic	0.20	1.2	4	10	29.6930	9.7384	2.361
4	20	Lines	0.25	1.6	5	15	37.4448	9.9855	1.222
5	20	Tri-Hexagon	0.30	2.0	6	20	45.1637	9.4658	3.500
6	40	Grid	0.15	1.2	5	20	28.9362	8.7673	2.556
7	40	Triangles	0.20	1.6	6	0	35.3763	9.2338	2.583
8	40	Cubic	0.25	2.0	2	5	35.2340	9.0676	3.306
9	40	Lines	0.30	0.4	3	10	21.9867	10.1953	2.028
10	40	Tri-Hexagon	0.10	0.8	4	15	21.1531	6.7758	2.278
11	60	Grid	0.20	2.0	3	15	38.9105	9.3022	2.528
12	60	Triangles	0.25	0.4	4	20	29.0139	10.2703	0.750
13	60	Cubic	0.30	0.8	5	0	36.5591	10.1640	2.778
14	60	Lines	0.10	1.2	6	5	30.8419	6.4420	1.944
15	60	Tri-Hexagon	0.15	1.6	2	10	31.8712	8.5373	1.167
16	80	Grid	0.25	0.8	6	10	54.9062	9.9132	2.000
17	80	Triangles	0.30	1.2	2	15	31.2713	10.1700	3.194
18	80	Cubic	0.10	1.6	3	20	32.3019	8.2395	3.389
19	80	Lines	0.15	2.0	4	0	42.7773	7.7538	1.750
20	80	Tri-Hexagon	0.20	0.4	5	5	32.8638	10.2032	2.139
21	100	Grid	0.30	1.6	4	5	46.2963	9.7172	2.611
22	100	Triangles	0.10	2.0	5	10	45.5006	7.0630	2.278
23	100	Cubic	0.15	0.4	6	15	42.2907	9.4370	1.861
24	100	Lines	0.20	0.8	2	20	40.5224	9.8110	1.750
25	100	Tri-Hexagon	0.25	1.2	3	0	37.7358	9.9765	1.972

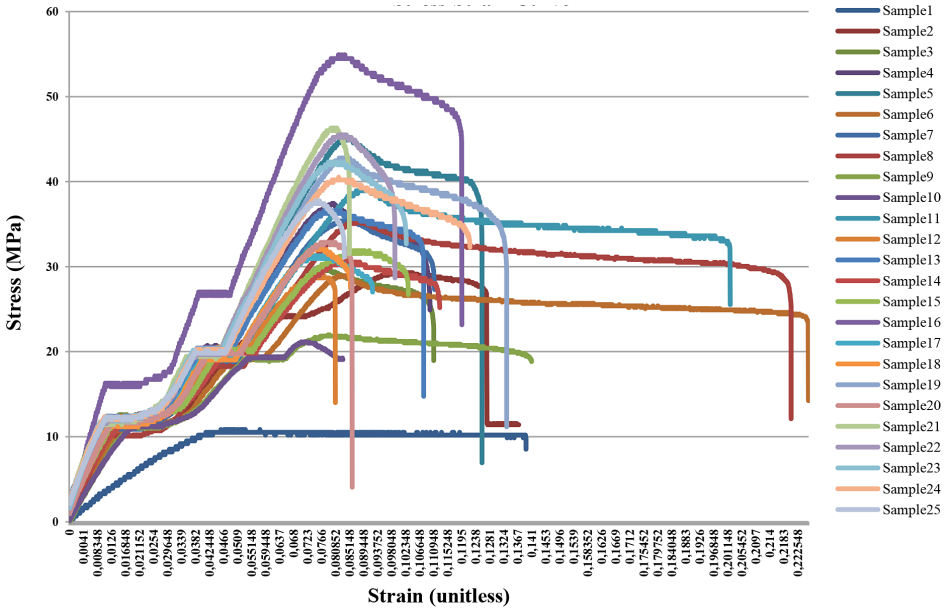

Fig. 6. Stress-strain curve for tensile specimen

thickness, 0.8 mm shell thickness, 6 top/bottom layer numbers, and 10% infill overlap produced by the printer was the strongest specimen with 55 MPa. In contrast, the 20% infill density, grid infill pattern, 0.1 mm layer thickness, 0.4 mm shell thickness, 2 top/bottom layers, and 0% infill overlap generated by FDM printer was the weakest specimen with 11 MPa, among other samples.

Results for tensile test

The ultimate tensile strengths of the specimens are displayed in Table 4. According to Figure 7, the study examined how the FDM processing parameters affected the ultimate tensile strengths of the specimens. The tensile strength is largely influenced by infill density. The experimental results presented for this study demonstrate that

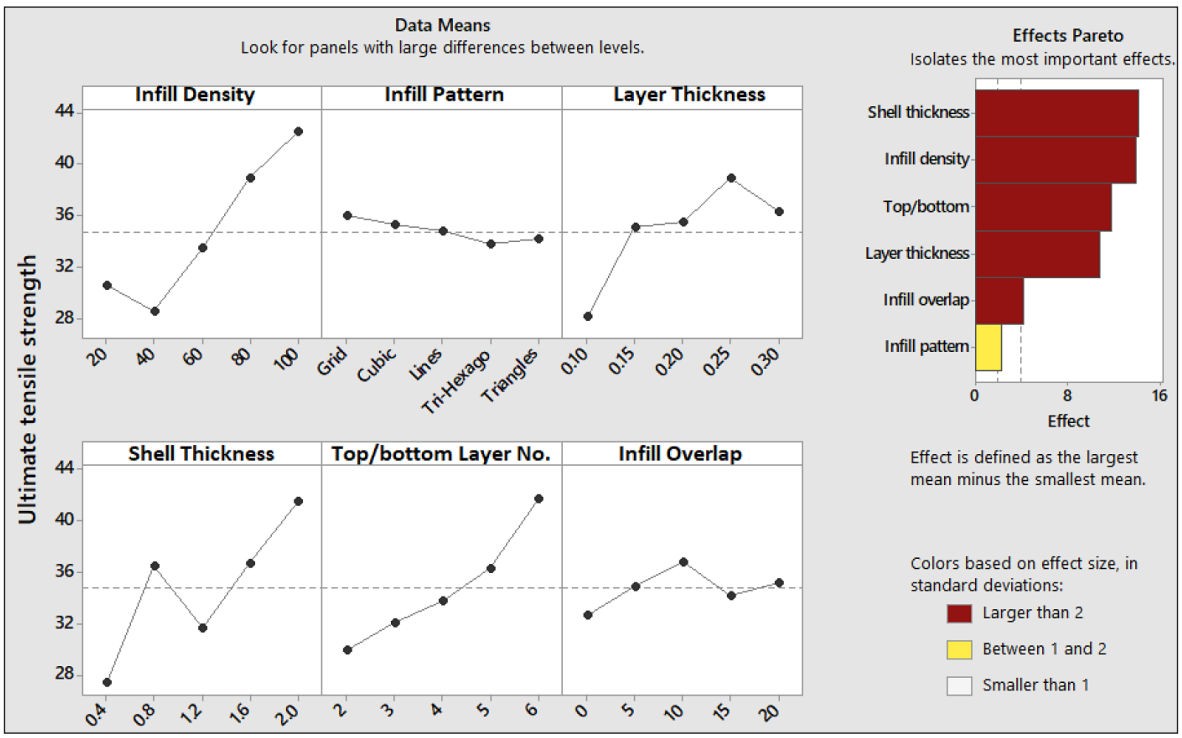

Fig. 7. Main effect plot for ultimate tensile strength, MPa

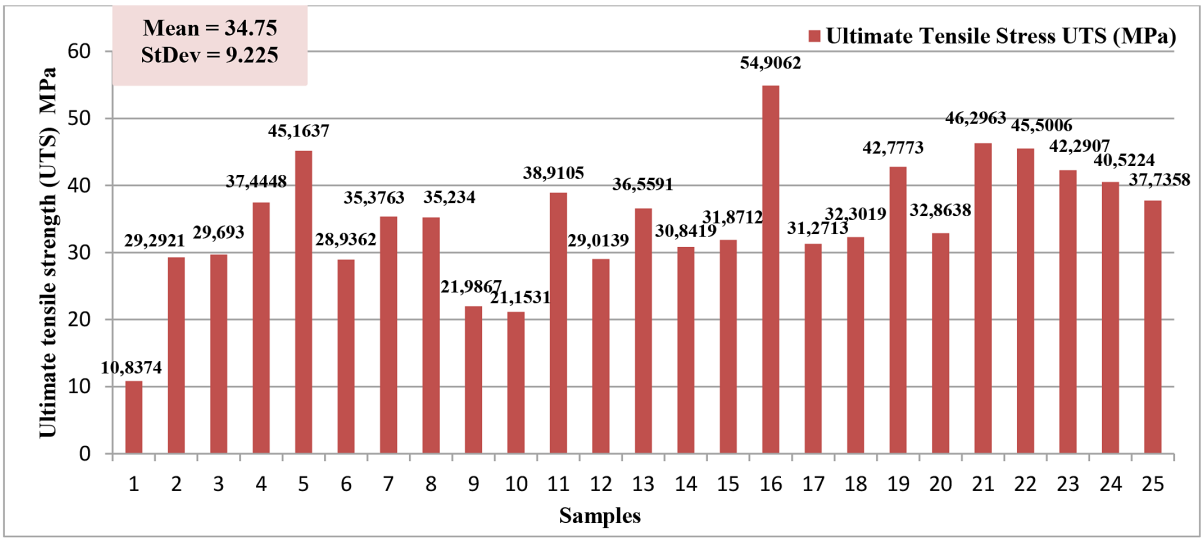

Fig. 8. Ultimate tensile strength variation with FDM parameters for printed parts

raising the infill density will increase tensile strength. As is clear, the specimen with an 80% infill density has a tensile strength of (55 MPa), which is approximately five times more than the specimen with a 20% infill density (11 MPa). The increase in infill density has been associated with an increase in the amount of material used. The maximum strength can be achieved with an infill density of 80%; however, this can have a negative impact on cost because it increases printing time and material consumption. Consequently, it would be crucial to determine the necessary infill density based on the type and application of the product.

Figure 8 displays the average tensile strength values (mean = 34.75) along with their corresponding standard deviations (StDev = 9.225). These values are presented to illustrate the variation in tensile strength among different samples under varying printing parameters. The grid pattern yielded the maximum tensile strength of 55 MPa among the five selected patterns. This can be explained by the fact that the grid pattern should have the optimal layer arrangement (in terms of layer bonding). Additionally, a layer thickness of 0.25 mm resulted in the highest tensile strength. This may be due to the fact that less material is extruded when using 0.25 mm layer thickness as opposed to 0.4 mm layer thickness, giving the filament more time to melt. On the other hand, as opposed to 0.1 mm layer thickness, 0.25 mm layer thickness has fewer layers, which lowers the risk of failure at the layers and improves the mechanical properties.

From Figure 7, between shell thickness and tensile strength, it is observed that the sample with a 2 mm shell thickness has the highest UTS value. Similarly, the specimen with 6 top/bottom layer number and 10% infill overlap has the highest UTS value. However, the specimens with 0.4 shell thickness have approximately the lowest UTS value. The UTS increases linearly with increasing top/bottom layer number. Between 5-6 changes of top/bottom layer number show the most significant effect in the UTS.

Results for surface roughness

The surface roughness criterion aids in the evaluation of fabricated parts functionality, which is as significant as the FDM parts strength and is influenced by the quality of the surface. The average surface roughness values, Ra, were determined by taking measurements perpendicular to the pull-out direction during a tensile test. The surface response of 25 FDM pieces was measured after they had been manufactured, as shown in Table 4. A line design with 60% infill density, 0.1 mm layer thickness, 1.2 mm shell thickness, 6 top/bottom layer numbers, and 5% infill overlap was found to produce the best results with a reduction in surface roughness from 10.2703 to 6.442 µm. The main effect plot for the effects of various machine parameters on Ra values is shown in Figure 9. The graphs show that layer thickness significantly influenced the surface roughness of the FDM pieces. This indicates that because the accuracy of the printed samples is decreasing and the layer is impacted by the step effect, the surface roughness increases proportionally with layer thickness. Figure 10 displays the average surface roughness values (mean

= 9.062) along with their corresponding standard deviations (StDev = 1.184). These values are presented to illustrate the variation in surface roughness among different samples under varying printing parameters. A 60% infill density, a triangle infill pattern, 0.25 mm layer thickness, 0.4mm shell thickness, 4 top/bottom layers, and 20% infill overlap were found to result in the worst surface quality for PLA parts, reaching 10.2703 µm, as shown in Figure 10. The poor quality of the triangle pattern was due to the design and classified layer.

Dimensional Accuracy results

Out of all the parameters that were examined, as shown in Table 4, shell thickness had the greatest effect on the specimen's tensile average deviation percentage. It was found that the smallest average percentage deviation was achieved with the machine parameters set as a grid pattern with 20% infill density, 0.1 mm layer thickness, 0.4 mm shell thickness, 2 top/bottom layer numbers, and 0% infill overlap. The percentage deviation decreased

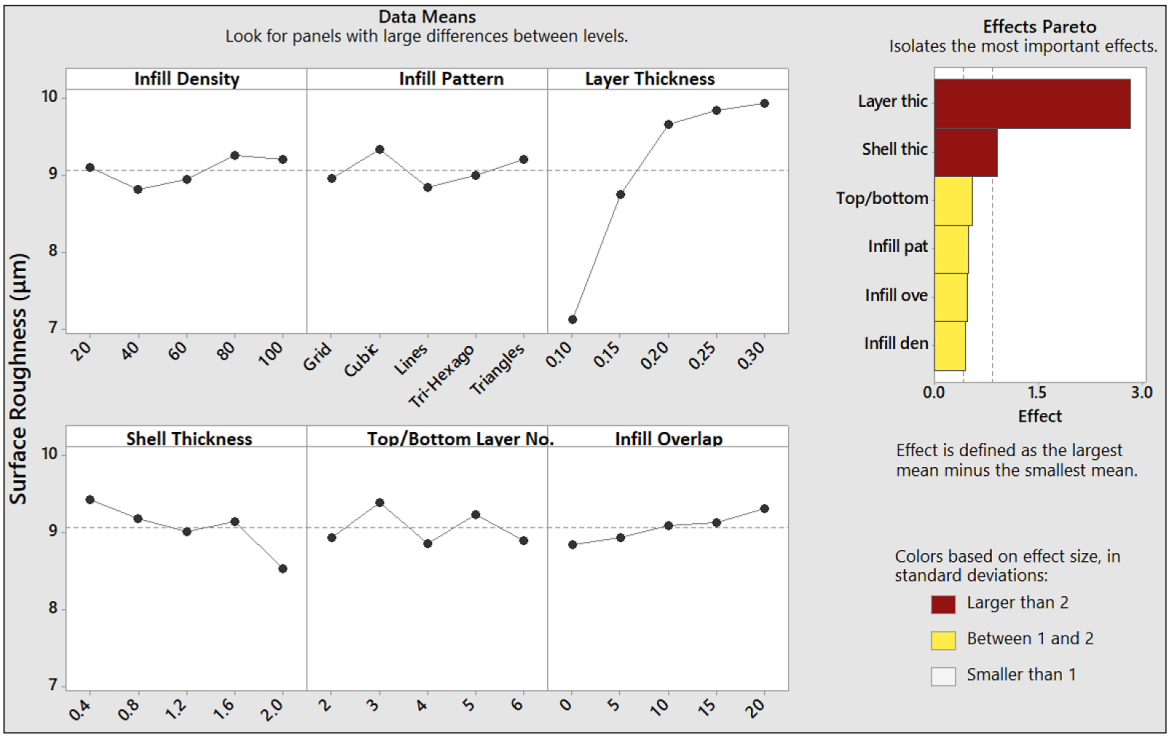

Fig. 9. Main effect plot for surface roughness

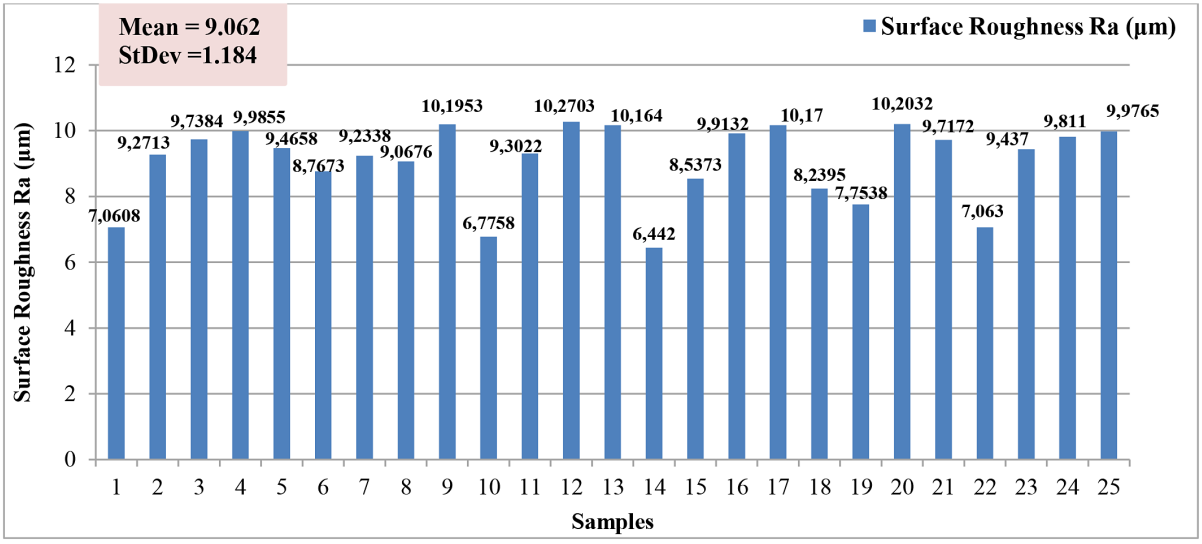

Fig. 10. Surface roughness variation with FDM parameters for printed parts

from 3.5% to 0.556%. The main effect plot in Figure 11 shows how various machine parameters affect tensile average deviation percentage values. The graphs show that the tensile average deviation percentage (dimensional accuracy) of the FDM parts was significantly influenced by shell thickness. This indicates that there is a minimum deviation for FDM parts. The deviation increases proportionally with shell thickness. Figure 12 displays the average tensile percentage deviation values (mean = 2.132) along with their corresponding standard deviations (StDev = 0.8064). These values are presented to illustrate the variation in tensile percentage deviation among different samples under varying printing parameters. A 20% infill density, a Tri-hexagon infill pattern, 0.3 mm layer thickness, 0.2 mm shell thickness, six top/bottom layers, and a 20% infill overlap had the highest average percentage variation for PLA parts, reaching 3.5%, as shown in Figure 12.

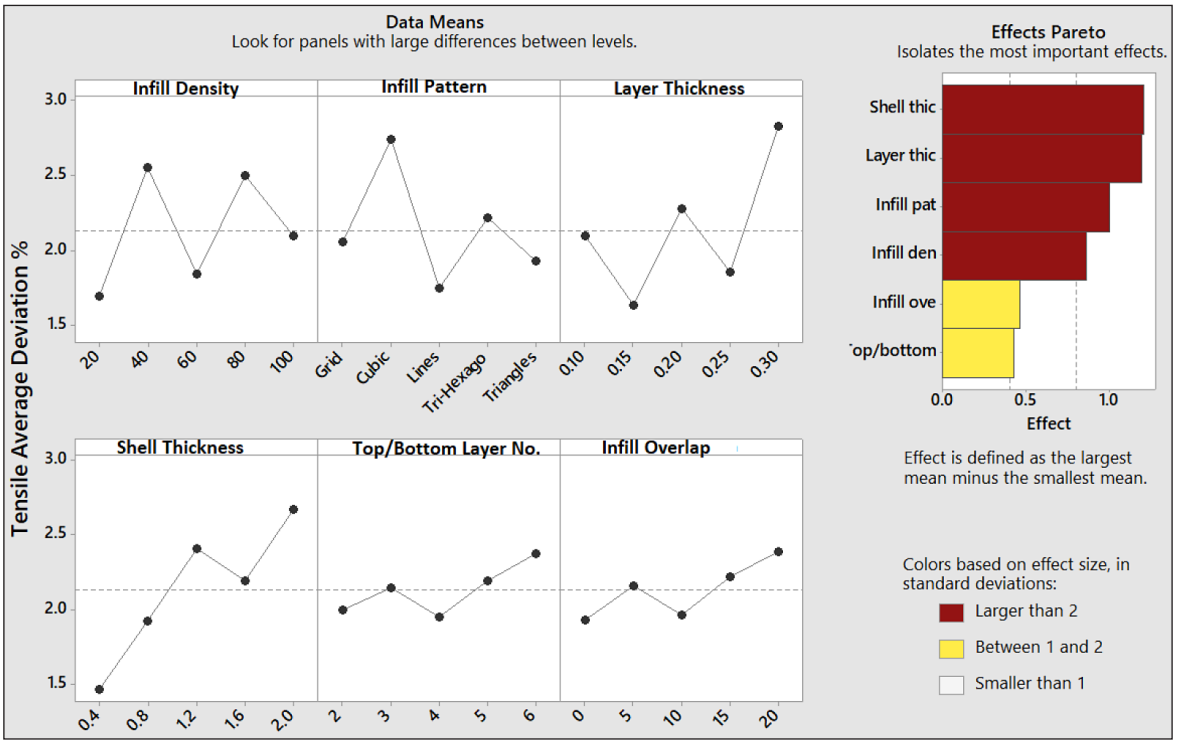

Fig. 11. Main effect plot for tensile average deviation %

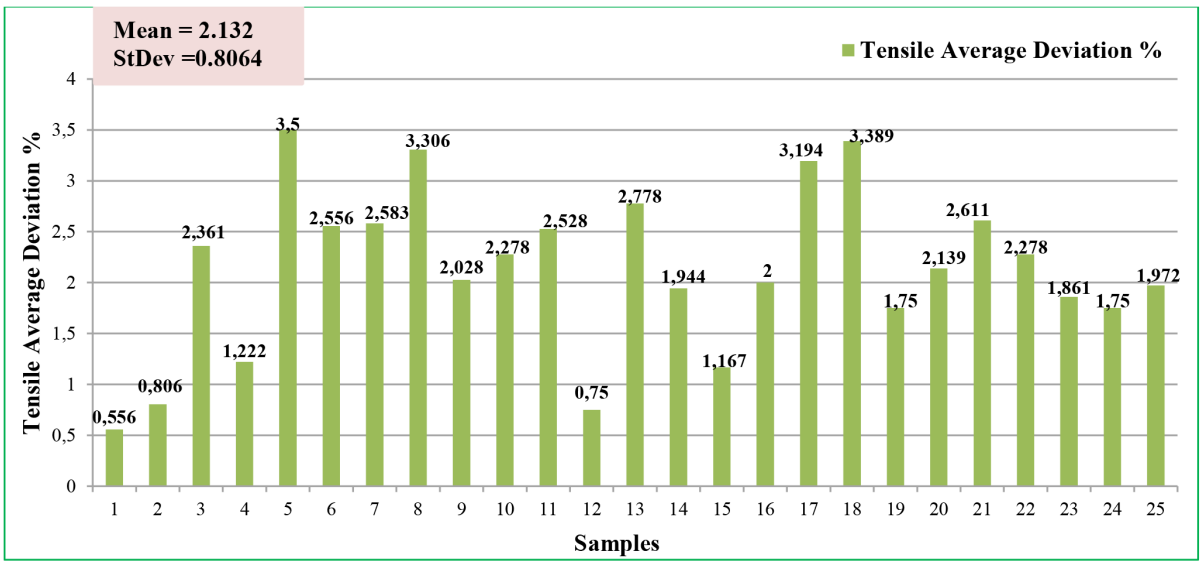

Fig. 12. Tensile average deviation % variation with FDM parameters for printed parts

Mechanical and physical properties changes of test specimens fabricated using different process parameters are given as interaction graphs in Figures 13, 14, and 15. Use the interaction plot to demonstrate how the value of the second categorical parameter affects the relationship between one categorical parameter and a continuous response. On the x-axis of this plot are the means for the levels of one parameter, and lines are shown separately for each level of another parameter. The lines in this interaction plot are not parallel. This interaction effect shows that the value of FDM parameters

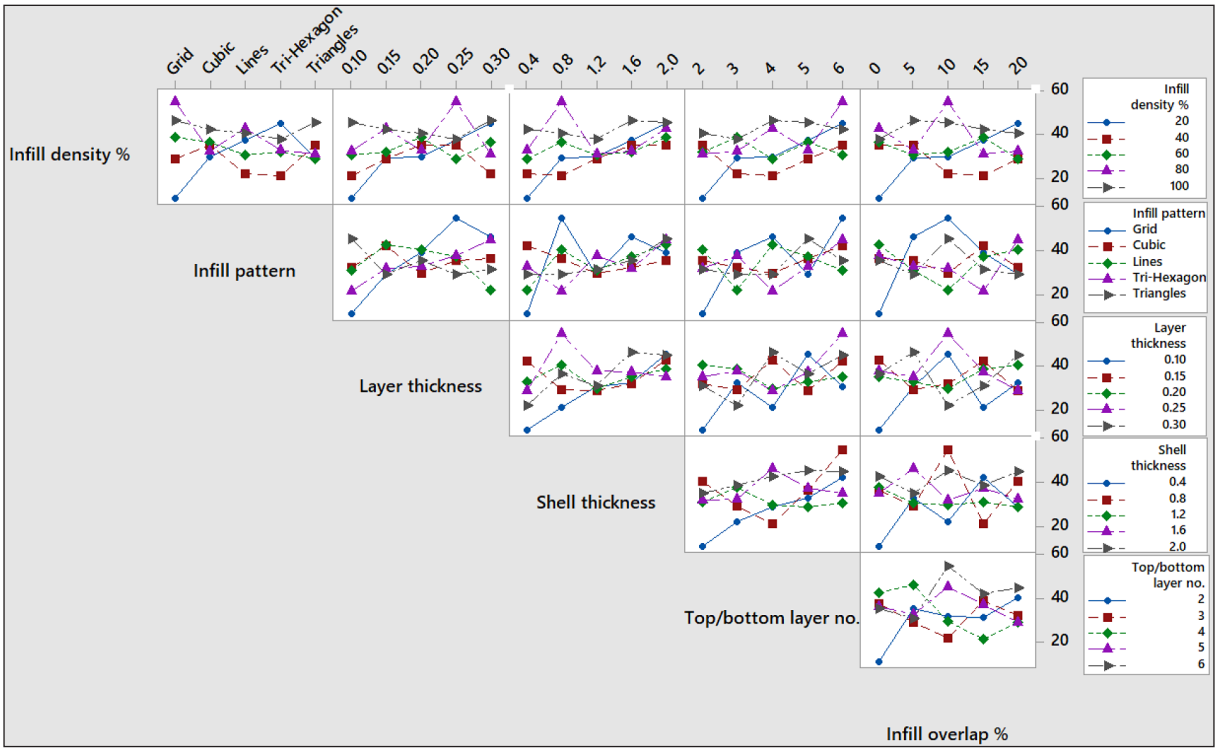

Fig. 13. Plot for tensile strength interaction

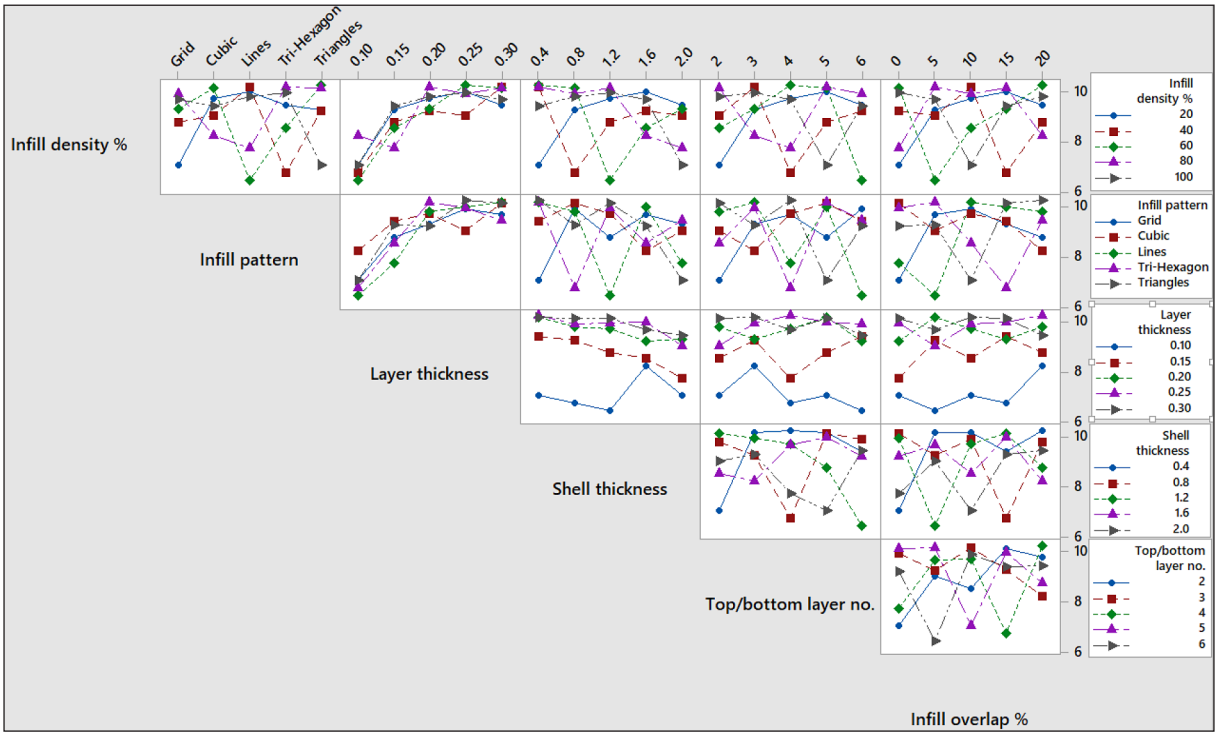

Fig. 14. Plot for surface roughness interaction

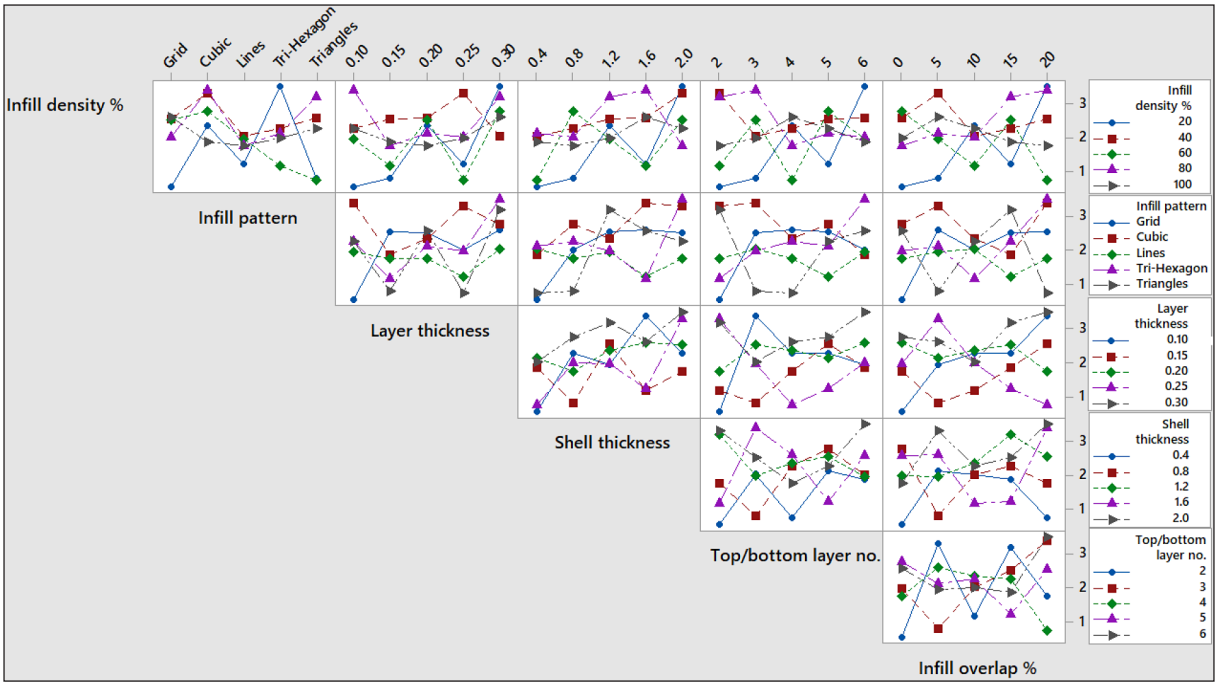

Fig. 15. Plot for tensile average deviation % interaction

Table 5. Percentage error for ultimate tensile strength, Ra, and tensile average deviation % of PLA parts

No.	Measured UTS (MPa)	Cubic predicted UTS (MPa)	Error %	Measured Ra (μm)	Cubic predicted Ra (μm)	Error %	Measured tensile average deviation %	Cubic predicted tensile average deviation %	Error %
1	10.8374	10.8654	0.26	7.0608	7.0631	0.03	0.556	0.5580	0.36
2	29.2921	29.3009	0.03	9.2713	9.2648	0.07	0.806	0.8108	0.6
3	29.6930	29.8092	0.39	9.7384	9.7316	0.07	2.361	2.3698	0.37
4	37.4448	37.5903	0.39	9.9855	9.9737	0.12	1.222	1.2350	1.06
5	45.1637	45.3442	0.40	9.4658	9.4510	0.16	3.500	3.5164	0.47
6	28.9362	29.0453	0.38	8.7673	8.7597	0.09	2.556	2.5633	0.29
7	35.3763	35.3948	0.05	9.2338	9.2220	0.13	2.583	2.5902	0.28
8	35.2340	35.3265	0.26	9.0676	9.0587	0.1	3.306	3.3148	0.27
9	21.9867	22.1054	0.54	10.1953	10.1878	0.07	2.028	2.0408	0.63
10	21.1531	21.225	0.34	6.7758	6.7675	0.12	2.278	2.2868	0.39
11	38.9105	38.9976	0.22	9.3022	9.2919	0.11	2.528	2.5363	0.33
12	29.0139	29.1059	0.32	10.2703	10.2581	0.12	0.750	0.7602	1.36
13	36.5591	36.6998	0.38	10.1640	10.1563	0.08	2.778	2.7884	0.37
14	30.8419	30.8978	0.18	6.4420	6.4305	0.18	1.944	1.9532	0.47
15	31.8712	31.9249	0.17	8.5373	8.5268	0.12	1.167	1.1769	0.85
16	54.9062	55.0463	0.26	9.9132	9.9051	0.08	2.000	2.0085	0.43
17	31.2713	31.3402	0.22	10.1700	10.1547	0.15	3.194	3.2064	0.39
18	32.3019	32.3946	0.29	8.2395	8.2255	0.17	3.389	3.3983	0.27
19	42.7773	42.8105	0.08	7.7538	7.7384	0.2	1.750	1.7598	0.56
20	32.8638	32.9584	0.29	10.2032	10.1951	0.08	2.139	2.1497	0.50
21	46.2963	46.4074	0.24	9.7172	9.7041	0.13	2.611	2.6213	0.39
22	45.5006	45.4722	0.06	7.0630	7.0415	0.30	2.278	2.2862	0.36
23	42.2907	42.4279	0.32	9.4370	9.4261	0.12	1.861	1.8701	0.49
24	40.5224	40.63	0.27	9.8110	9.7979	0.13	1.750	1.7636	0.78
25	37.7358	37.8045	0.18	9.9765	9.9640	0.13	1.972	1.9846	0.64

affects tensile strength, Ra, and dimensional accuracy. Figure 13 demonstrates that for 80% infill density, layer thickness is 0.25 mm, shell thickness is 0.8 mm, there are 6 top and bottom layers, and with 10% infill overlap, strength levels are higher.

Smooth surface texture can be obtained, as illustrated in Figure 14, when infill density is equal to 60%, lines pattern, layer thickness is 0.1 mm, shell thickness is 1.2 mm, there are 6 top and bottom layers, and there is 5% infill overlap.

It can be observed from Figure 15 that the minimum average tensile deviation results at 20% infill density, grid pattern, layer thickness of 0.1 mm, shell thickness of 0.4 mm, 2 top and bottom layers, and 0% infill overlap.

The value of the percentage error between measured and predicted responses of PLA parts was calculated according to equation 7. It has been shown from Table 5 that the maximum values of percentage error between measured and predicted UTS, Ra, and tensile average deviation % of PLA parts were 0.54%, 0.3%, and 1.36%, respectively, while the minimum values of percentage error between measured and predicted ultimate tensile strength (UTS), Ra, and tensile average deviation % of PLA parts were 0.03%, 0.03%, and 0.27%, respectively.

$$\text{Error } \% = \left| \left(\frac{\text{measured UTS} - \text{Predicted UTS}}{\text{measured UTS}} \right) * 100 \right| \quad (7)$$

CONCLUSIONS

The impact of FDM processing parameters on the tensile test mechanical characteristics, Surface roughness, and dimensional accuracy of FDM specimens was examined using Taguchi's L25 DOE. Prior to performing tensile testing, linear dimension measurements for the specimens' dimensional accuracy as well as surface profile measurements were carried out in accordance with the ASTM D683-type 4 standard for inspecting the specimens.

According to the work results on the mechanical properties of fabricated specimens, a higher infill density of 80%, a grid infill pattern, 0.25 mm layer thicknesses, 0.8 mm shell thicknesses, six top and bottom layers, and 10% infill overlap optimize the tensile strength of parts with a value of 55 MPa.

For the physical properties of the FDM specimens, the lines pattern with 60% infill density, 0.1 mm layer thickness, 1.2 mm shell thickness, 6 top/bottom layer numbers, and 5% infill overlap had the best surface profile result obtained in this work according to the selected parameters, with a value of (6.442 μm), however the expected Ra is based on reference [22] ranges from 1.779 μm to 3.979 μm for specimens. The triangles pattern, on the other hand, was the worst because of its design and inadequate adhesion.

It was found that the smallest average percentage deviation of 0.556% was achieved with the machine parameters set as a grid pattern with 20% infill density, 0.1 mm layer thickness, 0.4 mm shell thickness, 2 top/bottom layer numbers, and 0% infill overlap.

It has been shown from Table 4 that the maximum value of percentage error between measured and predicted ultimate tensile strength of PLA parts was 0.54%, while the minimum percentage error between measured and predicted ultimate tensile strength of PLA parts was 0.03%.

The maximum value of percentage error between measured and predicted surface roughness of PLA parts was 0.3%, while the minimum percentage error between measured and predicted surface roughness of PLA parts was 0.03%.

The maximum value of percentage error between measured and predicted Tensile average deviation % of PLA parts was 1.36%, while the minimum value of percentage error between measured and predicted tensile average deviation % of PLA parts was 0.27%.

Finally, it is obvious that it is impossible to maximize mechanical characteristics while minimizing physical properties when setting the values of FDM parameters. In order to enhance the strength of printed parts, a grid infill pattern, 80% infill density, layer thicknesses of 0.25 mm, a shell thickness of 0.8 mm, six top and bottom layers, and 10% infill overlap are recommended as FDM parameters. On the other hand, the line pattern with 60% infill density, 0.1 mm layer thickness, 1.2 mm shell thickness, 6 top/bottom layer numbers, and 5% infill overlap must be specified to reduce the surface roughness. Whereas 20% infill density, 0.1 mm layer thickness, 0.4 mm shell thickness, 2 top/bottom layer numbers, and 0% infill overlap must be selected as FDM parameters to minimize tensile average deviation%. As a result, it is required to sacrifice mechanical or physical characteristics in order to optimize another property or to carry out a multi-objective optimization.

REFERENCES

1. Trevor J.S., Mike A., Mark W., et al. 3D systems' technology overview and new applications in manufacturing, engineering, science, and education. 3D Printing and Additive Manufacturing 2014; 1(3): 169–176. https://doi.org/10.1089/3dp.2014.1502
2. G.D. Goh, Y.L. Yap, H.K.J. Tan, et al. Process-structure-properties in polymer additive manufacturing via material extrusion: a review. Critical Reviews in Solid State and Materials Sciences 2019; 45(2): 1–21. https://doi.org/10.1080/10408436.2018.1549977
3. Vigneshwaran S., Oisik D., Rasoul E.N., et al. Polymer Recycling in Additive Manufacturing: an Opportunity for the Circular Economy. Materials Circular Economy 2020; 2(11). https://doi.org/10.1007/s42824-020-00012-0
4. Adam M.P., Mark R., Joshua M.P., et al. Wood Furniture Waste-Based Recycled 3-D Printing Filament. Forest Products Journal 2018; 68(1): 86-95. https://doi.org/10.13073/FPJ-D-17-00042
5. Mohd N. A., Mohamad R. I., Mastura M. T., et al. Application of Taguchi Method to Optimize the Parameter of Fused Deposition Modeling (FDM) Using Oil Palm Fiber Reinforced Thermoplastic Composites. Polymers, 2022; 14(11): 2140. https://doi.org/10.3390/polym14112140
6. M. Kam, A. İpekçi, Ö. Şengül. Taguchi Optimization of Fused Deposition Modeling Process Parameters on Mechanical Characteristics of PLA+ Filament Material. Scientia Iranica B 2022; 29(1): 79-89. http://doi.org/10.24200/sci.2021.57012.5020
7. Maria F.J., Tahseen F.A., Abdullah F.H. The effect of Infill Pattern on Tensile Strength of PLA Material in Fused Deposition Modeling (FDM) Process. Engineering and Technology Journal 2022; 40 (21): 1723-1730. http://doi.org/10.30684/etj.2021.131733.1054
8. Tahseen F.A., Khalida K.M., Hind B.A. The effect of FDM Process Parameters on the Compressive Property of ABS Prints. Journal of Hunan University (Natural Sciences) 2022; 49(7): 154-162. https://doi.org/10.55463/issn.1674-2974.49.7.17
9. R.A. Hamid, N.K. Marnyi, F.H. Hamezah, et al. Effect of different PLA filament colours and process parameters towards the tensile strength of 3d printed parts. Proceedings of Malaysian Technical Universities Conference on Engineering and Technology (MUCET), 2021, 168-169.
10. Selim B., Hatice V.Ö., Mehmet M.S. Comparison of Mechanical Properties of 3D-Printed Specimens Manufactured Via FDM with Various Inner Geometries. Journal of the Institute of Science and Technology 2021; 11(2): 1444-1454. https://doi.org/10.21597/jist.772977
11. Mohd R.A., Nor A.R., Siti N.A.M., et al. Properties of 3D printed structure manufactured with integrated pressing mechanism in FDM. Journal of Mechanical Engineering Research and Developments 2021; 44(2): 122-131.
12. Mohammadreza L.D. and Mohd K.A.M.A. The effects of Combined Infill Patterns on Mechanical Properties in FDM Process. Polymers 2020; 12(12): 2792. https://doi:10.3390/polym12122792
13. Can T., Junwei L., Yang Y., et al. Effect of process parameters on mechanical properties of 3D printed PLA lattice structures. Composites Part C: Open Access 2020; 3(100076). https://doi.org/10.1016/j.jcomc.2020.100076
14. Muhammad S.C. and Aleksander C. Evaluating FDM Process Parameter Sensitive Mechanical Performance of Elastomers at Various Strain Rates of Loading. Materials 2020; 13(14). http://doi:10.3390/ma13143202
15. Teng C.Y. and Chin H.Y. Morphology and Mechanical Properties of 3D Printed Wood Fiber/Polylactic Acid Composite Parts Using Fused Deposition Modeling (FDM): The effects of Printing Speed. Polymers 2020; 12(6). http://doi:10.3390/polym12061334
16. Cristina V., Liviu M., Mihai M., et al. Effect of manufacturing parameters on tensile properties of FDM printed specimens. In: Proc. of 1st Mediterranean Conference on Fracture and Structural Integrity, MedFract1, Procedia Structural Integrity, 2020, 313–320. https://doi.org/10.1016/j.prostr.2020.06.040
17. Mst F.A., S.H. Masood, Pio I., et al. Effects of part build orientations on fatigue behaviour of FDM-processed PLA material. Progress in Addittive Manufacturing 2015; 1: 21–28.
18. Galantucci L.M., F. Lavecchia, G. Percoco. Experimental study aiming to enhance the surface finish of fused deposition modeled parts. CIRP Annals 2009; 58(1): 189–192.
19. Sohail G., G. Hussain, Aaqib A., et al. Mechanical performance of honeycomb sandwich structures built by FDM printing technique. Journal of Thermoplastic Composite Materials 2021; 1-19. https://doi.org/10.1177/0892705721997892
20. Chamil A., Pimpisut S., Anura F. Optimization of fused deposition modeling parameters for improved PLA and ABS 3D printed structures. International Journal of Lightweight Materials and Manufacture 2020; 3: 284-297. https://doi.org/10.1016/j.ijlmm.2020.03.003
21. Krishna M.A., Pritish S., Dinesh B., et al. Analyzing the Impact of Print Parameters on Dimensional Variation of ABS specimens printed using Fused Deposition Modelling (FDM). Sensors International 2022; 3. https://doi.org/10.1016/j.sintl.2021.100149
22. Maria F.J., Abdullah F.H., Tahseen F.A. Investigation of the Effect of Surface Roughness and Dimensional Accuracy on the Layer Thickness of PLA Parts Produced by the FDM Process. Progress in Engineering Technology V 2023; 183:19–29.